Characterization of the anterior cingulate's role in the at-risk mental state using graph theory

Lord, L.-D.; Expert, P.; Turkheimer, F.E.; Howes, O.; McGuire, P.; Lambiotte, R.; Bose, S.K.; Hyde, S.; Allen, P.

Published in:
NeuroImage

DOI:
10.1016/j.neuroimage.2011.02.012

Publication date:
2011

Document Version
Publisher's PDF, also known as Version of record

NeuroImage 56 (2011) 1531–1539

Contents lists available at ScienceDirect

NeuroImage

journal homepage: www.elsevier.com/locate/ynimg

Characterization of the anterior cingulate's role in the at-risk mental state using graph theory ☆

Louis-David Lord [a,e,*], Paul Allen [b], Paul Expert [c], Oliver Howes [a,b,d], Renaud Lambiotte [c], Philip McGuire [b], Subrata K. Bose [d], Samuel Hyde [e], Federico E. Turkheimer [a,d]

[a] Department of Experimental Medicine, Imperial College London, UK
[b] Institute of Psychiatry, King's College London, UK
[c] Institute for Mathematical Science, Imperial College London, UK
[d] MRC Clinical Sciences Center, Hammersmith Hospital, London, UK
[e] Athinoula A. Martinos Center for Biomedical Imaging, Massachusetts General Hospital, Harvard Medical School, Boston, USA

ARTICLE INFO

Article history:
Received 28 October 2010
Revised 12 January 2011
Accepted 2 February 2011
Available online 22 February 2011

ABSTRACT

The onset of positive symptoms in schizophrenia is often preceded by a prodromal phase characterized by neurocognitive abnormalities as well as changes in brain structure and function. Increasing efforts have been made to identify individuals at elevated risk of developing schizophrenia, as early intervention may help prevent progression towards psychosis. The present study uses functional MRI and graph theoretical analysis to characterize the organization of a functional brain network in at-risk mental state patients with varying symptoms assessed with the PANSS and healthy volunteers during performance of a verbal fluency task known to recruit frontal lobe networks and to be impaired in psychosis. We first examined between-groups differences in total network connectivity and global network compactness/efficiency. We then addressed the role of specific brain regions in the network organization by calculating the node-specific "betweeness centrality", "degree centrality" and "local average path length" metrics; different ways of assessing a region's importance in a network. We focused our analysis on the anterior cingulate cortex (ACC); a region known to support executive function that is structurally and functionally impaired in at-risk mental state patients. Although global network connectivity and efficiency were maintained in at-risk patients relative to the controls, we report a significant decrease in the contribution of the ACC to task-relevant network organization in at risk subjects with elevated symptoms (PANSS $\geq$ 45) relative to both the controls and the less symptomatic at-risk subjects, as reflected by a reduction in the topological centrality of the ACC. These findings provide evidence of network abnormalities and anterior cingulate cortex dysfunction in people with prodromal signs of schizophrenia.

Introduction

Schizophrenia and other chronic psychotic disorders affect nearly 1% of the world's population. The onset of these disorders is usually preceded by a prodromal phase characterized by cognitive impairments, mood alterations and attenuated psychotic symptoms (Yung and McGorry, 1996). In recent years operationalised criteria have been developed that identify individuals in the prodrome to the first psychotic episode. These criteria require the recent onset of specific symptoms or clinical features, termed an 'at risk mental state' (ARMS), and are associated with functional impairment. Individuals with an ARMS display a need for care (Wood et al., 2008) and have an ultra high risk of developing a psychotic disorder, predominantly schizophrenia, within two years.

Converging evidence indicates that schizophrenia is associated with disordered connectivity between brain systems, which impairs functional integration (Friston, 2002). Firstly, diffusion tensor imaging (DTI) studies have provided evidence of disruption in white matter tracts in first-episode psychosis patients in comparison to age-matched controls, which indicates that abnormalities in structural connectivity are present at illness onset and are not a secondary consequence of medication, or illness duration (Gasparotti et al., 2009; Hao et al., 2006; Price et al., 2007; Segal et al., 2010). Similar abnormalities have also been reported in ARMS subjects (Bloemen et al., 2009; Peters et al., 2009).

Secondly, functional connectivity, defined by the cross-correlation in the activity time-series of spatially remote brain regions, has been found to be reduced in frontal cortical regions during the performance of executive tasks in both chronic and first-episode patients (Benetti et al., 2009; Boksman et al., 2005; Crossley et al., 2009; Lawrie et al.,

☆ Funding: the project has been funded in part by the EPSRC grant EP/E049451/1 and MRC grant U.1200.04.007.00001.01.
* Corresponding author at: 2 Hawthorne Place, Suite 5B, Boston, MA, 02114, USA. Fax: +1 617 726 4078.
E-mail address: LDL@nmr.mgh.harvard.edu (L.-D. Lord).

1053-8119/$ – see front matter © 2011 Elsevier Inc. All rights reserved.
doi:10.1016/j.neuroimage.2011.02.012

2002; Spence et al., 2000). More recently, functional and effective connectivity have also been examined in ARMS individuals at high clinical risk of developing psychosis. During performance of functional tasks, connectivity between pairs of ROIs or within small a priori networks of interest has been reported to be preserved in some cases (Allen et al., 2010; Crossley et al., 2009), although impairments have also been identified (Benetti et al., 2009; Crossley et al., 2009). It is difficult to reconcile these results due to notable differences in the experimental tasks being employed, and in the brain regions under study.

Graph theory (GT) provides powerful mathematical tools to study the behavior of complex systems of interacting elements (Bullmore and Sporns, 2009), and has more recently been used to study the topological properties of brain networks. The first step in the study of a functional brain network using GT is to define the network nodes in terms of anatomically defined regions. It is then necessary to establish a continuous measure of association between the nodes (i.e. inter-regional correlations in activity) and generate a matrix compiling all the associations between pairs of nodes at a set statistical threshold. Parameters of interest can then be calculated from the network representation of the system. Specific graph metrics can provide insight into either the *local* or the *distributed* interactions occurring in the brain, either of which may be affected in a disease state (Bassett and Bullmore, 2009).

Recent studies have notably used fMRI and graph theoretical methods to study the behavior of functional brain networks in chronic schizophrenia patients. Several abnormalities were revealed by these analyses. First, at the level of global network function, schizophrenia patients show disrupted 'small world' network organization in comparison to healthy controls (Alexander-Bloch et al., 2010; Liu et al., 2008; Lynall et al., 2010). Small-world architecture is thought to satisfy the brain's balance between local specialization and global interaction in a cost-effective manner for information transfer. It was also found that schizophrenia patients have a more diverse and less integrated profile of functional connectivity than healthy individuals, where fewer nodes emerge as 'functional hubs' (regions of high connectivity) and the strength of functional connections is more uniformly distributed across the brain (Lynall et al., 2010). These results were in agreement with an earlier graph theoretical investigation of anatomical connectivity in SZ where a loss of topological hierarchy was also reported (Bassett et al., 2008). In addition to these impairments in global network topology, several regional differences in network organization between SZ patients and controls have been reported including changes in degree centrality and local clustering in the prefrontal, parietal and temporal areas (Alexander-Bloch et al., 2010; Liu et al., 2008; Lynall et al., 2010). Although graph theoretical methods have identified many important differences in the functional architecture of chronic SZ patients, we believe the present study is the first to use graph theory to characterize network topology in ARMS patients at elevated risk of developing psychosis.

In the present study, fMRI data from individuals with an ARMS and age-matched controls were collected during performance of a verbal fluency task, known to recruit frontal lobe networks (Hill et al., 2004), and to be impaired in psychosis (Allen et al., 1993; Goldberg et al., 1988). The goal of the study was to use graph theoretical analysis to characterize the functional connectivity in ARMS subjects while performing the verbal fluency (VF) task. To investigate the degree to which abnormalities in network organization were related to state factors we divided the ARMS subjects into two groups according to the severity of their symptoms at the time of scanning. Symptom severity increases during the progression of the prodrome (Yung et al., 2005) so, while imperfect, this exploratory approach aimed to identify individuals who were in the early and late prodrome.

ARMS subjects with more pronounced symptoms (ARMS-H), less pronounced symptoms (ARMS-L) and healthy controls were first compared on three global network metrics: network density, global average path length and global betweenness-centrality. Network density is a measure of the total connectivity of a network, while the global average path length and global betweenness-centrality are global measures of the compactness of a network, and can be related to its efficiency. Then, in order to address the role of specific brain regions in the network organization, we examined the regional analogs of these global measures: the local degree centrality (DC), local betweenness-centrality (BC), and local average path-length (L). BC, DC, and L are different ways of assessing a region's importance in the organization of a network (Freeman, 1977, 1979).

In this work, we were specifically interested in examining the role of the anterior cingulate cortex (ACC) in the network under study. Schizophrenia and the at-risk mental state involve deficits in executive function and information processing (Eastvold et al., 2007; Hawkins et al., 2004), and the ACC is known to support these functions as part of the default mode and executive networks (Broyd et al., 2009; Buckner et al., 2008; Carter et al., 1999; Garrity et al., 2007; McKiernan et al., 2003). Functional abnormalities have been reported in the ACC of chronic SZ and ARMS subjects both in the resting state (Garrity et al., 2007) and during performance of executive tasks (Broome et al., 2009; Meyer-Lindenberg et al., 2001; Rubia et al., 2001). Furthermore, alterations in gray-matter volumes have been reported in the ACC of ARMS subjects (Goldstein et al., 1999; Ohnuma et al., 1997).

We therefore selected 19 regions of interest from the default mode and executive networks as the nodes for graphical analysis. Functional connectivity data were derived from the activity time-series between the nodes and used to create a graphical model of the network for each group.

We hypothesized that the ACC's topological importance in the network would be decreased in ARMS subjects relative to controls, which would translate into a smaller BC value for this region. We also expected ARMS-H individuals to show an even greater reduction in the BC of the ACC than the ARMS-L group. Because betweenness centrality is often correlated with other centrality measures, we conducted follow-up analyses to investigate group differences in degree centrality (DC) and local average path length (L) in the ACC. We expected to find a corresponding decrease of the degree-centrality and an increase in local average path length of the ACC in ARMS subjects relative to controls. Such results would be consistent with a reduction in the topological importance of this region in the ARMS groups. We finally examined specific ACC connectivity patterns across the three groups.

Materials and methods

Participants

Fifty-five subjects (22 healthy volunteers and 33 with an ARMS in the prodrome of schizophrenia) participated in the study. All the subjects were right-handed according to the Lateral Preference Inventory, native English speakers, and had no prior history of neurological illness or substance dependence. ARMS subjects were recruited via OASIS (Outreach and Support in South London), a clinical service for people at high risk of developing psychosis. Diagnosis of an At Risk Mental State was made using the Comprehensive Assessment of At Risk Mental States (CAARMS) (Yung et al., 2005). One or more of the following criteria had to be met for inclusion in the study: attenuated psychotic symptoms, brief limited intermittent psychotic symptoms in the past year, or a recent decline in function together with either a family history of psychosis in a first degree relative or schizotypal personality disorder. All ARMS subjects were experiencing attenuated psychotic symptoms, while five had also experienced brief limited intermittent psychotic symptoms. Six had a family history together with a recent decline in function.

Healthy controls were recruited from the local community through advertisements. Control subjects were excluded if they had a history of

neurological or psychiatric disorder, substance abuse, or received prescription medication.

The mean age of ARMS subjects was 24.2 ± 5.3 (mean ± SD, 21 males and 12 females), and that of the comparison subjects was 25.5 ± 4.6 (15 males and 7 females). There was no significant difference between the groups in terms of age [$t(53) = 0.89$, $p = 0.38$]. The self-reported ethnicity of the at-risk group was 22 White British, 4 Black, 4 Asian, and 3 of mixed origins. The control group consisted of 14 White British, 7 Black, and 1 of Asian origin.

Neuropsychological measures

Premorbid IQ for all subjects was estimated using the National Adult Reading Test (NART) (Nelson, 1982). On the day of scanning, psychopathology in prodromal subjects was assessed using the Positive and Negative Symptoms Scale (PANSS) (Kay et al., 1987).

Experimental task

Functional MRI data were acquired while subjects performed a verbal fluency task (Broome et al., 2009). Subjects were instructed to overtly generate a word in response to a visually presented letter. They were asked not to use names, repeat words, or to use grammatical variations of a previously used word. The letters were presented at a rate of one letter every 4 s. There were two conditions which differed in difficulty. In the 'easy' condition, the letters C, P, S, T, and L were presented, while the 'hard' condition consisted of the five-letter set: I, F, O, N, and E. Each condition was presented in blocks lasting 28 s, with seven presentations of a given letter per block, and five blocks for each condition. The experimental condition alternated with a control condition, also presented in blocks of 28 s, in which the subjects were presented with the word 'rest' at 4 s intervals and were instructed to repeat the word overtly. Verbal responses were recorded with a microphone compatible with MRI apparatus. Responses were considered incorrect when participants passed on a given letter, and when the word recorded was a repetition or grammatical variation of a previous word. To maximize the statistical power of the functional connectivity analysis (see below), data from the 'easy', 'hard', and 'rest' VF conditions were collapsed together.

Image acquisition and processing

Functional MRI data were acquired at the Institute of Psychiatry at the Maudsley Hospital, London, on a GE Sigma 1.5-T system (General Electric, Milwaukee). Verbal fluency was studied using a T2-weighted echoplanar image sequence (TR = 4000 ms, TE = 40 ms) with each acquisition compressed into the first 2000 ms of the repetition time, in order to create a 2000 ms silent period in which subjects could articulate a response in the absence of scanner noise. Compressed acquisition sequences were also used to reduce motion artifact due to head movement during articulation. One hundred and eight brain volumes were collected from each subject. Each volume contained 22 axial 5 mm slices with a 0.5 mm gap between each slice. This sequence delivered a voxel resolution of 3.75 × 3.75 × 5.5 mm. The University of Oxford's fMRIB software library (FSL) was used for image processing.

Spatial smoothing (5 mm) was performed on the raw images, and a high pass filter was applied (0.01 Hz). Each subject's fMRI data was registered to a standard space by FSL's linear registration algorithm (FLIRT) (Jenkinson et al., 2002). Motion correction was performed using MCFLIRT, FSL's intramodal motion correction tool (Jenkinson et al., 2002). Task-elicited BOLD time-series were extracted from bilateral regions-of-interest (ROI) defined by the Harvard-Oxford Cortical Structural Atlas. Regional time-series were calculated by taking the mean of the voxel time-series within each ROI. ROI templates were applied to the standard space used for registration. Nuisance variables (ventricles and white matter noise) were extracted from the raw time-series, and excluded from the analysis. The whole-brain signal was added as a covariate of non-interest. The medial prefrontal cortex, anterior cingulate cortex (ACC), parahippocampal areas (Parahipp.), posterior cingulate (PCC), and precuneus are all part of the well characterized default mode network (Buckner et al., 2008) that has been implicated in schizophrenia (Broyd et al., 2009; Garrity et al., 2007; McKiernan et al., 2003). Additionally, BOLD time-series were extracted from ROIs known to support executive function, and for which functional impairment has been reported in schizophrenia (Hill et al., 2004; Tan et al., 2007): the insular cortex, inferior frontal gyrus (IFG-pT/pO), middle frontal gyrus (MFG), ventromedial prefrontal cortex (vmPFC), and the cuneate cortex. Importantly, some default-mode regions such as the ACC and medial prefrontal cortex are also part of the executive networks (Carter et al., 1999; Fuster, 2001).

Functional connectivity analysis

The fMRI data were organized into three groups: healthy control subjects, ARMS subjects with low symptoms based on PANSS total scores (ARMS-L; PANSS 30–44) and ARMS subjects with high symptoms (ARMS-H; PANSS ≥ 45). The ARMS-L ($n = 17$) and ARMS-H ($n = 16$) subgroups were determined according to a median split of the total PANSS score distribution. For each subject, functional connectivity was determined by performing partial correlations between fMRI time-series for all pair-permutations of nodes. Partial correlations were preferred over regular bivariate correlations since correlation coefficients between two nodes may be statistically significant even if the nodes are not directly functionally connected, but simply are on parallel computing streams. Random effect analysis was performed by transforming partial correlation coefficients derived for each node pair for each subject into normalized Z-scores via a Fisher transform. For each group, the Z-scores were averaged and then transformed into p-values for testing. To control the family-wise error rate at the $\alpha = 0.05$ level, the set of p-values derived for the network for each group was corrected using the Hochberg procedure for multiple comparison compounded by the p-plot estimator of the number of true-null hypotheses (Turkheimer et al., 2001). This multiple comparison correction procedure is the most powerful to date to control for the FDR when the proportion of non-null hypotheses is large, as is expected when analyzing functional brain networks (Hwang, 2010). All functional connectivity methods described above are contained in the HamNet software (Imperial College London) that is coded as a toolbox for Matlab (The Mathworks, Natick, MA).

Graph theoretical analysis

Regional (node-specific) centrality measures

Graph theoretical analysis was used to compare the control, ARMS-L and ARMS-H connectivity patterns. In graph theory, a graph is defined as a set of N nodes connected by L edges. In our analysis, the graphs have been produced by considering the 19 ROIs as nodes and joining them with an edge if their correlation was found to be statistically significant by the HamNet analysis. By construction, the graphs that we have considered are unweighted, undirected, and do not contain self-loops. Their adjacency matrix A is therefore symmetric, and its elements $A_{i,j}$ are equal to 1 if nodes i and j are connected and zero otherwise. This operation was performed for each group of subjects, thereby leading to three different networks defined on the same set of nodes. All three networks were made of a single component.

To quantify the topological importance of the nodes, we first used a standard graph metric called the "betweenness-centrality" (BC) (Freeman, 1977, 1979). The importance of a node in a graph is

usually associated with a certain notion of its centrality, as central nodes play a key role by serving as hubs for network traffic and by influencing directly or indirectly a large number of vertices. The *betweenness-centrality* of a node measures how many of the shortest paths between all other node pairs pass through it and is a measure of its importance when routing information in the network. For a node k, it is defined as:

$$BC(k) = \sum_{\substack{i\neq j\neq k \\ i,j=1}}^{N} \frac{\sigma_{i,j}(k)}{\sigma_{i,j}}.$$

where $\sigma_{i,j}(k)$ is the length of the shortest path going from node i to node j through node k, and $\sigma_{i,j}$ is the total number of shortest paths going from node i to node j. The betweenness-centrality of a node depends on the global organization of the graph, and not only on the direct neighborhood of the node. The length of the shortest path is defined as the minimal number of edges one has to go through to join two nodes. In a graph, there can be several shortest paths possible between two nodes, and if the nodes belong to two unconnected components, the shortest path is infinite by definition.

In addition to the betweenness-centrality, we calculated two other regional centrality measures for each node; the *degree centrality* (DC) and *local average path length* (L). Degree centrality is a measure of the total number of connections that a node has. It therefore depends on the direct neighborhood of the node, and, contrary to BC, is independent of the overall topology of the rest of the network. BC and DC are in general different even if both metrics are typically correlated (Barthememy, 2004), particularly in dense networks where "mean-field" descriptions are expected to hold (Pugliese and Castellano, 2009), and differences between local and global metrics tend to be minor (Sinatra et al., 2010). Although defined locally, DC is a measure of the global importance of nodes for key dynamical processes such as diffusion and synchronization when the network is undirected (Batty and Tinkler, 1979). For a node k, degree is defined as:

$$DC(k) = \sum_{i=1}^{N} A_{k,i}.$$

Local average path length (L) is defined as the average shortest path between a node i and the other nodes constituting the network where $\sigma_{i,j}$ is the shortest path between i and j :

$$L(i) = \frac{1}{(N-1)} \sum_{j=1}^{N} \sigma_{i,j}.$$

Thus, the local average path length of a node, like BC, depends on both the direct neighborhood of a node and the global organization of the graph. All other things kept constant, a reduction in the topological centrality of a node is associated with an *increase* in its local average path length.

Global network measures

To characterize the overall behavior of each network, we used the global analogs of the regional network metrics described above: the network density, global average path length, and the global betweenness-centrality.

We calculated the density (ρ) of each network by counting the number of significant functional connections between pairs of nodes, and dividing it by the total number of possible connections:

$$\rho = \frac{1}{N(N-1)} \sum_{i,j=1}^{N} A_{i,j}.$$

We examined the compactness of each network by calculating the global average path length (l), which gives information about the average number of links that separate pairs of nodes in the network and is thus a measure of the diameter of the network. The smaller the global average path length, the more compact (and efficient) the network is (Latora and Marchiori, 2001). The average path length is defined as the average of the shortest paths $\sigma_{i,j}$ between each pair of nodes:

$$\bar{l} = \frac{1}{N(N-1)} \sum_{i=1}^{N} \sum_{\substack{j=1 \\ j\neq 1}}^{N} \sigma_{i,j}.$$

The global betweenness-centrality was also used to examine the compactness of each network, thus being another measure of their diameter. This metric was calculated by averaging the local values of BC:

$$\overline{BC} = \frac{1}{N} \sum_{k=1}^{N} BC(k) = \frac{1}{N} \sum_{k=1}^{N} \sum_{\substack{i\neq j\neq k \\ i,j=1}}^{N} \frac{\sigma_{i,j}(k)}{\sigma_{i,j}}$$

All graphs were plotted with Visone software (http://visone.info/index). The values for all metrics were computed with Visone and the free Matlab toolbox BCT (Rubinov and Sporns, 2009). To facilitate comparison between groups whose total connectivities may be slightly different, the values of the BC, DC and L metrics for each node are given as percentage of the total metric value for each graph.

Between-groups statistical analysis of GT data

The statistical significance of the variation of network densities, global average path lengths, global betweenness-centrality and node properties (BC, DC, L) between two groups was assessed by application of a permutation test. Two groups (x and y) were selected from the overall set comprising controls, ARMS-L and ARMS-H. For each node we computed the difference in a given metric (Met) that we denote:

$$D_{Met}^{Obs}(i) = Met_x^{Obs}(i) - Met_y^{Obs}(i) \quad (1)$$

where $i = 1,\ldots,19$ is the label of the nodes. We then randomized the labels of the subjects constituting the two original groups and thus obtained two new groups of the same size as the original ones. We then applied HamNet to obtain two new connectivity graphs and recomputed the metric differences:

$$D_{Met}^{Rnd(n)}(i) = Met_{x'}^{Rnd(n)}(i) - Met_{y'}^{Rnd(n)}(i) \quad (2)$$

where $i = 1,\ldots,19$, x' and y' are two randomized version of x and y and $n = 1,\ldots,N$ is the label of the randomization round. In this study, we set $N = 500$. The p-values were computed for each difference and each node as follows for one-tailed (Eq. (3a)–(3b)) or two-tailed tests (Eq. (3c)), respectively:

$$p-val_{Met}(i) = Nbr\left(D_{Met}^{Obs}(i) > D_{Met}^{Rnd(n)}(i)\right) / N, if\ D_{Met}^{Obs} > 0 \quad (3a)$$

and

$$p-val_{Met}(i) = Nbr\left(D_{Met}^{Obs}(i) < D_{Met}^{Rnd(n)}(i)\right) / N, if\ D_{Met}^{Obs} < 0, \quad (3b)$$

$$p-val_{Met}(i) = Nbr\left(D_{Met}^{Obs}(i) > D_{Met}^{Rnd(n)}(i)\right) / N \quad (3c)$$

By doing so, we counted the number of times the observed difference between two groups was higher than the differences produced under the null hypothesis that the two groups were exchangeable. The same procedure was applied to the network density, global average path length, and global betweenness-centrality metrics, but

Table 1
Betweenness-centrality (BC) values — percent. Betweenness-centrality (BC) values for each node in each network under study, expressed as a percentage of the total betweenness-centrality of the corresponding network.

ROI#	ROI	Control	ARMS-L	ARMS-H
1	ACC	19.0	13.4	3.7
2	Cuneate-L	0.1	3.4	0.4
3	vmPFC	9.2	4.5	4.0
4	IFGpO-L	12.2	1.5	9.9
5	IFGpT-L	3.4	6.1	10.1
6	Insula-L	1.1	9.1	2.8
7	MFG-L	4.9	12.7	11.5
8	Parahipp.-L	2.1	0.6	6.3
9	PCC	1.2	2.2	1.6
10	Precuneus-L	9.5	2.7	10.3
11	Sup. Parietal-L	0.9	4.2	2.1
12	Cuneus-R	0.1	9.7	0.4
13	IFGpO-R	2.1	11.8	5.0
14	IFGpT-R	2.7	0.3	2.6
15	Insula-R	5.5	2.7	5.4
16	MFG-R	15.8	4.2	5.4
17	Parahipp.-R	1.7	5.8	4.8
18	Precuneus-R	5.8	3.2	9.3
19	Sup. Parietal-R	2.7	1.8	4.3

with a single value for each network at each stage, as these measures are not node-dependent.

Results

Characteristics of the participants

There was no significant difference in premorbid IQ between the ARMS-L (106 ± 3; mean $\pm$ SEM), ARMS-H (100 ± 2.8), and controls (107 ± 2); [$F(2, 50) = 2.29$, $p = 0.11$]. The same three groups also did not show a difference in performance on the verbal fluency task [$F(2, 52) = 0.91$, $p = 0.41$] and committed similar numbers of errors: 13 ± 2 (controls), 15 ± 2 (ARMS-L), 18 ± 3 (ARMS-H); mean $\pm$ SEM.

The ARMS-L group had a mean PANSS rating of 38 ± 1 in comparison to 57 ± 2 for ARMS-H. This difference was significant [$t(31) = 7.14$, $p < 0.01$].

Network density, global average path length, global betweenness-centrality

Network densities for the control, ARMS-L and ARMS-H groups were: 39%, 39%, and 36%, respectively. None of the between group comparisons for network density reached statistical significance (all p-val > 0.50, two-tailed). Similarly, control (1.66), ARMS-L (1.64), and ARMS-H (1.73) groups showed no significant difference in global average path length (all p-val > 0.50, two-tailed). Global betweenness-centrality was also maintained across the three experimental groups: control (11.9%), ARMS-L (11.5%), ARMS-H (13.1%) (all p-val > 0.45, two-tailed). Having statistically similar density values allows for the direct comparison of raw values for local metrics (BC, DC, *L*). However, we preferred to present the results as percentage of the total metric value for each graph in order to better reflect the relative importance of a node in a given network, thus controlling for variations in the absolute size of the system.

ACC betweenness-centrality for the ARMS-L, ARMS-H and control networks

Table 1 contains the BC values for each node in each network, and these same values are represented graphically in Fig. 2. In both the control network and ARMS-L network, the ACC was the region with the highest BC relative to the other nodes. No significant between-groups difference in BC was observed in the ACC for the ARMS-L vs.

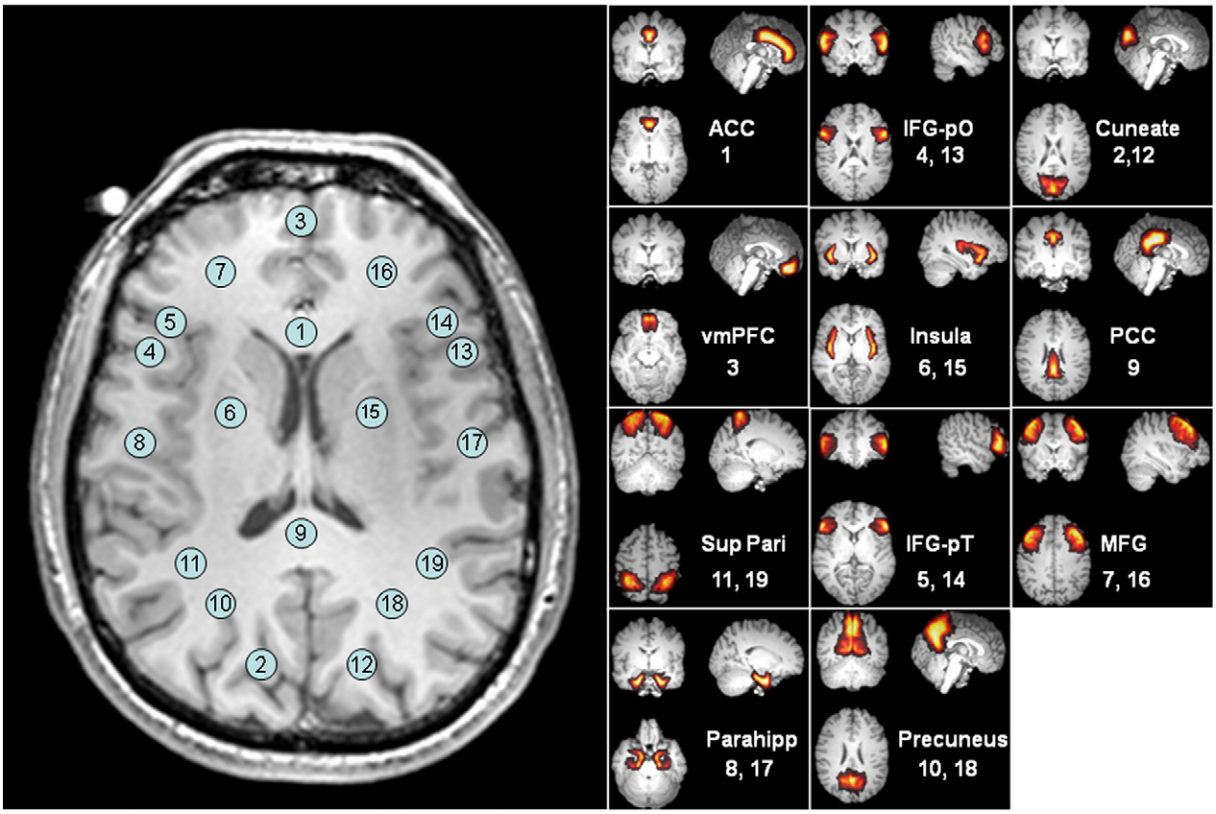

Fig. 1. Regions of interest for the functional connectivity analysis. Schematic representation of the 19 regions comprising the network considered in the functional connectivity analysis, together with their probabilistic activation maps from FSL's Harvard–Oxford structural atlas.

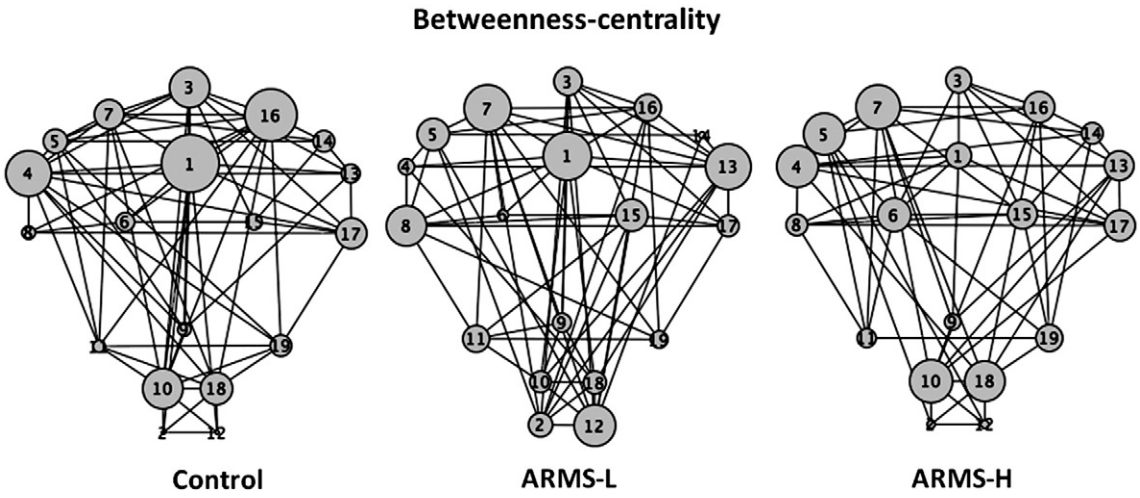

Fig. 2. Visual representation of the networks and BC values. Graphical representation of the networks for the control, ARMS-L and ARMS-H groups. Each edge represents a significant functional connection between a pair of nodes. The surface area of each node is directly proportional to its *betweenness-centrality* value, expressed as a proportion of the total metric value of the corresponding network. The nodes are presented on a 2-dimensional X–Y plane that reflects their relative positions in the brain from a top-down perspective as showed in Fig. 1.

control comparison. However, the BC of the ACC was significantly lower in the ARMS-H group (3.7%) than both the ARMS-L (13.4%) ($p = 0.05$; one-tailed) and control (19.0%) networks (p-val = 0.03; one-tailed).

ACC degree-centrality for the ARMS-L, ARMS-H and control networks

In the control and ARMS-L networks, no other node had greater DC than the ACC. However, this was not the case in the ARMS-H network where many nodes had greater degree centrality than the ACC. ACC degree centrality did not significantly differ between the ARMS-L and control networks. However, the ARMS-L group (8.2%) had significantly greater ACC degree centrality than the ARMS-H group (4.9%) (p-val = 0.04; one-tailed) while a near-significant difference was observed in the control (8.1%) vs. ARMS-H comparison ($p = 0.06$, one-tailed). See Table 2 and Fig. 3.

Table 2
Degree-centrality (DC) values — percent. Degree-centrality (DC) values for each node in each network under study, expressed as a percentage of the total degree centrality of the corresponding network.

ROI#	ROI	Control	ARMS-L	ARMS-H
1	ACC	8.1	8.2	4.9
2	Cuneate-L	2.9	6.0	3.3
3	vmPFC	7.4	6.0	4.9
4	IFGpO-L	8.1	3.7	6.6
5	IFGpT-L	5.9	5.2	5.7
6	Insula-L	2.9	6.0	4.9
7	MFG-L	6.6	7.5	7.4
8	Parahipp.-L	2.9	3.0	5.7
9	PCC	4.4	4.5	3.3
10	Precuneus-L	7.4	4.5	6.6
11	Sup. Parietal-L	5.1	4.5	4.1
12	Cuneus-R	2.9	6.7	3.3
13	IFGpO-R	4.4	7.5	5.7
14	IFGpT-R	3.7	2.2	4.9
15	Insula-R	5.1	4.5	5.7
16	MFG-R	8.1	6.0	5.7
17	Parahipp.-R	2.9	5.2	5.7
18	Precuneus-R	5.9	5.2	6.6
19	Sup. Parietal-R	5.1	3.7	4.9

ACC local average path length for the ARMS-L, ARMS-H and control networks

In line with the regional betweenness-centrality and degree-centrality findings, the ACC had a lower local average path length (L) value than all other nodes under study in the ARMS-L (4.46%) and control (4.40%) networks; indicative of high topological centrality. This was not the case in the ARMS-H network where L in the ACC (5.42%) was significantly greater than in both the ARMS-L ($p = 0.03$, one-tailed) and control groups ($p = 0.04$, one-tailed).The ARMS-L and control groups, on the other hand, did not show a difference in local average path length in the ACC ($p = 0.48$, one-tailed). See Table 3.

Supplementary Tables S1, S2 and S3 contain the raw values for BC, DC and L for each node in each network. Supplementary Tables S4, S5 and S6 contain the results of between-group comparison tests ran on the percent values of BC, DC and L. Supplementary Tables S7, S8 and S9 show the results of between-group comparisons of BC, DC and L using raw values, rather than percent values.

ACC connectivity patterns in ARMS-L, ARMS-H and control networks

ACC connectivity patterns were very similar in the ARMS-L and control networks. Not only did the ARMS-L and control networks count the same total number of significant functional connections involving the ACC (11), but 9 of those 11 connections were identical in both networks. Moreover, the 5 significant functional connections involving the ACC in the ARMS-H network were all found in *both* the ARMS-L and control networks.

Discussion

The present results demonstrate important differences in the organization of the functional network recruited during verbal fluency in ARMS-H subjects in comparison to healthy controls and ARMS-L subjects. In the control and ARMS-L groups, the anterior cingulate cortex (ACC) is highly central to the overall connectivity of the network under study as reflected by its elevated degree centrality (DC) and betweenness centrality (BC) values, as well as its low regional average path length (L) relative to other nodes in the network. However, for the ARMS-H group, BC and DC are significantly reduced in the ACC, L is significantly increased, and this region no

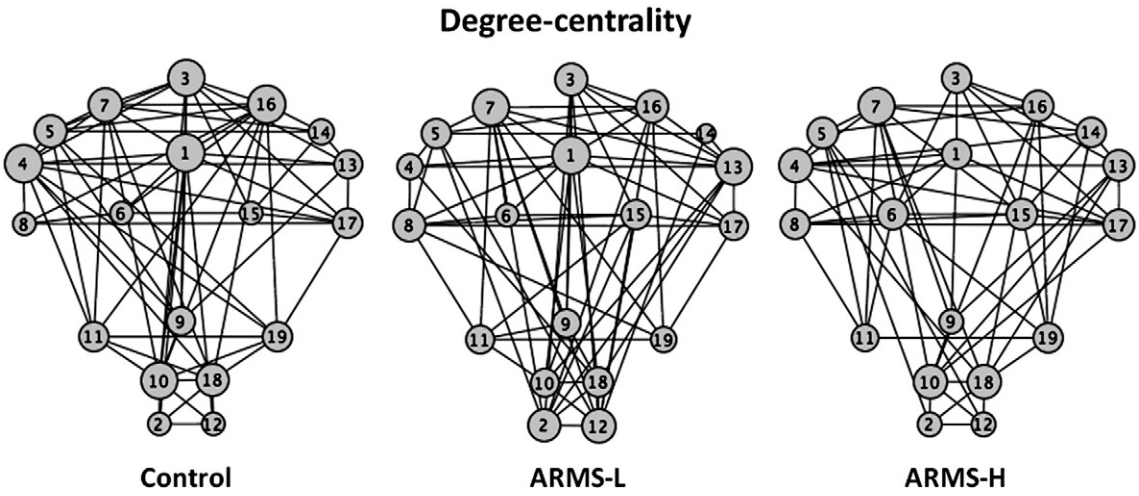

Fig. 3. Visual representation of the networks and DC values. Graphical representation of the networks for the control, ARMS-L and ARMS-H groups. Each edge represents a significant functional connection between a pair of nodes. The surface area of each node is directly proportional to its *degree-centrality* value, expressed as a proportion of the total metric value of the corresponding network. The nodes are presented on a 2-dimensional X–Y plane that reflects their relative positions in the brain from a top-down perspective as showed in Fig. 1.

longer occupies a central role in the functional network topology. This suggests that the ACC may no longer support the efficient routing of information during verbal fluency in ARMS-H subjects.

This finding is particularly interesting in light of the large body of research implicating the ACC in SZ and the at-risk mental state. The ACC is structurally connected to the prefrontal cortex and largely involved in executive control in situations where errors are likely to be made (van Veen and Carter, 2002). Because many aspects of the cognitive and executive dysfunction reported in schizophrenia are normally regulated by the ACC (Carter et al., 1999), it is not surprising that structural and functional abnormalities have been reported in the ACC of psychotic patients.

The ACC shows significant volumetric reductions in schizophrenia patients in comparison to healthy controls (Goldstein et al., 1999; Ohnuma et al., 1997), and fMRI studies have showed that it is under-activated during performance of various executive tasks (Meyer-Lindenberg et al., 2001; Rubia et al., 2001). In ARMS individuals, total ACC gray matter volumes are closer to those reported in first-episode psychosis patients than controls (Borgwardt et al., 2007) and neuro-functional ACC deficits have also been reported during verbal fluency (Broome et al., 2009). During VF task performance, ARMS subjects have been reported to show abnormal ACC activation relative to healthy volunteers (Allen et al., 2010; Broome et al., 2009). Furthermore, two earlier graph theoretical investigations of resting-state functional connectivity have reported significantly reduced regional clustering in the ACC of schizophrenia patients relative to healthy controls (Alexander-Bloch et al., 2010; Lynall et al., 2010).

Since network densities are remarkably similar across the three groups under study, it can be inferred that the observed decrease in ACC betweenness centrality in the ARMS-H network is not driven by a global, nonspecific loss of functional connectivity in the more symptomatic subjects. Importantly, no other node shows a greater decrease in betweenness centrality than the ACC when contrasting the ARMS-H network with both the ARMS-L and control networks. Because between-group differences in ACC betweenness-centrality were consistently associated with corresponding differences in degree centrality, it is more likely that a loss of functional connectivity *specific to the* ACC underlies its decrease in BC.

Of particular importance, not only is the degree centrality of the ACC preserved in ARMS-L subjects relative to controls (both counted 11 connections involving the ACC), but *specific* ACC *connectivity patterns* are also conserved. Nearly all the functional connections involving the ACC in the control network (9 of 11) are also found in the ARMS-L network. This suggests similarities in the cognitive strategy employed by these two groups to accomplish the task, and comparable ACC demand for cognitive control over the brain areas recruited by the task. Furthermore, each of the 5 significant functional connections found in the ACC in the ARMS-H network are present in *both* the ARMS-L and control networks. This suggests that the ACC of ARMS-H subjects specifically loses *useful* connections, and does not appear to make new aberrant connections.

A question that follows is how ARMS-H individuals maintain task performance in the absence of normal ACC connectivity. Our finding that global average path length and global betweenness-centrality are maintained in the ARMS-H group suggests that the network is capable of adjusting to the ACC impairment in order to maintain its overall efficiency. Although we did not test specific a priori hypotheses about possible compensatory mechanisms, our results indicate that regions other than the ACC become highly central to the network topology in the ARMS-H group. For instance, the BC of the left MFG region is substantially greater (although not significantly different) in ARMS-H and ARMS-L subjects relative to the control network. Interestingly, the left MFG is normally engaged during verbal fluency in healthy

Table 3
Local average path length (L) values — percent. Local average path length (L) values for each node in each network under study, expressed as a percentage of the total metric value of the corresponding network.

ROI#	ROI	Control	ARMS-L	ARMS-H
1	ACC	4.40	4.46	5.42
2	Cuneate-L	6.34	5.00	6.27
3	vmPFC	4.58	5.00	5.42
4	IFGpO-L	4.40	5.54	4.75
5	IFGpT-L	5.28	5.18	4.92
6	Insula-L	5.99	5.00	5.59
7	MFG-L	4.75	4.64	4.58
8	Parahipp.-L	5.63	5.89	5.08
9	PCC	5.28	5.54	5.59
10	Precuneus-L	4.58	5.36	4.92
11	Sup. Parietal-L	5.28	5.54	5.42
12	Cuneus-R	6.34	4.82	6.27
13	IFGpO-R	5.28	4.64	5.08
14	IFGpT-R	5.81	6.61	5.42
15	Insula-R	5.11	5.36	4.92
16	MFG-R	4.40	5.00	5.08
17	Parahipp.-R	6.34	5.18	5.25
18	Precuneus-R	5.11	5.36	4.75
19	Sup. Parietal-R	5.11	5.89	5.25

subjects (Curtis et al., 1998; Spence et al., 2000), and is not differentially activated in ARMS and control subjects during VF task performance (Broome et al., 2009).

That the ACC's importance in the functional architecture of the network under study is significantly reduced in more symptomatic at-risk subjects (ARMS-H) relative to both controls and less symptomatic at-risk subjects (ARMS-L) is indicative of the ACC's possible involvement in disease progression. Previous studies have implicated the ACC in the transition towards psychosis. Notably, a longitudinal study by Pantelis and colleagues (Pantelis et al., 2003) showed significantly greater reductions in ACC gray matter volumes in ARMS subjects who had developed psychosis in comparison to those who had not after a 12 month follow-up period. Similar findings were reported in a more recent cross-sectional analysis that compared at-risk subjects who later transitioned to psychosis to those who did not (Borgwardt et al., 2007); significantly decreased ACC gray matter volumes were found in the converted group relative to the non-converts. Thus, there is convincing evidence from structural imaging studies that brain changes specific to the transition towards psychosis may be taking place in the ACC of ARMS individuals. Here we extend these findings by showing that there are also functional alterations in the ACC that underlie the network dysfunction seen in the most symptomatic ARMS subjects. Future work will attempt to identify what specific differences in the ACC contribute to reductions in its topological importance.

It is important to note that a number of ARMS subjects from the present cohort have developed psychosis in the months following the scan. However, as follow-up of the entire cohort remains to be completed, it would be premature to analyze these separately. The categorization into ARMS-L and ARMS-H groups is imperfect, but evidence indicates it reflects clinically meaningful progression (Yung et al., 2005). Longitudinal studies are needed to determine if there is a progressive impairment in the network during the progression from the early through the late prodromal phase to first psychotic episode.

We therefore provide evidence, for the first time, that the betweenness centrality, degree centrality and local average path length of a key region within a functional brain network are altered in the ARMS. Traditionally, in order to study the functional involvement of a ROI in a brain network, correlations between activity time-series of neighboring areas have been examined. In such cases, limitations arise from the fact that pairs of ROIs must be selected a priori, and the overall topology of the network of interest is ignored. Importantly, the combination of graph metrics and analyses used in the present study provides the notable advantages of: allowing for the identification of region-specific contributions to information routing, and taking into account the overall organization of the system of interest.

In conclusion, these findings indicate that network abnormalities particularly involving the anterior cingulate cortex are present in people with at risk mental states prior to the onset of psychosis.

Appendix A. Supplementary data

Supplementary data to this article can be found online at doi:10.1016/j.neuroimage.2011.02.012.

References

Alexander-Bloch, A.F., et al., 2010. Disrupted modularity and local connectivity of brain functional networks in childhood-onset schizophrenia. Front. Syst. Neurosci. 4, 147.

Allen, H.A., et al., 1993. Negative features, retrieval processes and verbal fluency in schizophrenia. Br. J. Psychiatry 163, 769–775.

Allen, P., et al., 2010. Cingulate activity and fronto-temporal connectivity in people with prodromal signs of psychosis. Neuroimage 49, 947–955.

Barthememy, M., 2004. Betweenness centrality in large complex networks. Eur. Phys. J. B 38, 163–168.

Bassett, D.S., Bullmore, E.T., 2009. Human brain networks in health and disease. Curr. Opin. Neurol. 22, 340–347.

Bassett, D.S., et al., 2008. Hierarchical organization of human cortical networks in health and schizophrenia. J. Neurosci. 28, 9239–9248.

Batty, M., Tinkler, K., 1979. Symmetric structure in spatial and social processes. Environ. Plann. B. 6, 3–27.

Benetti, S., et al., 2009. Functional integration between the posterior hippocampus and prefrontal cortex is impaired in both first episode schizophrenia and the at risk mental state. Brain 132, 2426–2436.

Bloemen, O.J., et al., 2009. White-matter markers for psychosis in a prospective ultra-high-risk cohort. Psychol. Med. 1–8.

Boksman, K., et al., 2005. A 4.0-T fMRI study of brain connectivity during word fluency in first-episode schizophrenia. Schizophr. Res. 75, 247–263.

Borgwardt, S.J., et al., 2007. Regional gray matter volume abnormalities in the at risk mental state. Biol. Psychiatry 61, 1148–1156.

Broome, M.R., et al., 2009. Neural correlates of executive function and working memory in the 'at-risk mental state'. Br. J. Psychiatry 194, 25–33.

Broyd, S.J., et al., 2009. Default-mode brain dysfunction in mental disorders: a systematic review. Neurosci. Biobehav. Rev. 33, 279–296.

Buckner, R.L., et al., 2008. The brain's default network: anatomy, function, and relevance to disease. Ann. NY Acad. Sci. 1124, 1–38.

Bullmore, E., Sporns, O., 2009. Complex brain networks: graph theoretical analysis of structural and functional systems. Nat. Rev. Neurosci. 10, 186–198.

Carter, C.S., et al., 1999. The contribution of the anterior cingulate cortex to executive processes in cognition. Rev. Neurosci. 10, 49–57.

Crossley, N.A., et al., 2009. Superior temporal lobe dysfunction and frontotemporal disconnectivity in subjects at risk of psychosis and in first-episode psychosis. Hum. Brain Mapp. 30, 4129–4137.

Curtis, V.A., et al., 1998. Attenuated frontal activation during a verbal fluency task in patients with schizophrenia. Am. J. Psychiatry 155, 1056–1063.

Eastvold, A.D., et al., 2007. Neurocognitive deficits in the (putative) prodrome and first episode of psychosis. Schizophr. Res. 93, 266–277.

Freeman, L., 1977. A set of measures of centrality based on betweenness. Sociometry 40, 35–41.

Freeman, L., 1979. Centrality in social networks: conceptual clarification. Soc. Networks 1, 215–239.

Friston, K.J., 2002. Dysfunctional connectivity in schizophrenia. World Psychiatry 1, 66–71.

Fuster, J.M., 2001. The prefrontal cortex — an update: time is of the essence. Neuron 30, 319–333.

Garrity, A.G., et al., 2007. Aberrant "default mode" functional connectivity in schizophrenia. Am. J. Psychiatry 164, 450–457.

Gasparotti, R., et al., 2009. Reduced fractional anisotropy of corpus callosum in first-contact, antipsychotic drug-naive patients with schizophrenia. Schizophr. Res. 108, 41–48.

Goldberg, T.E., et al., 1988. Performance of schizophrenic patients on putative neuropsychological tests of frontal lobe function. Int. J. Neurosci. 42, 51–58.

Goldstein, J.M., et al., 1999. Cortical abnormalities in schizophrenia identified by structural magnetic resonance imaging. Arch. Gen. Psychiatry 56, 537–547.

Hao, Y., et al., 2006. White matter integrity of the whole brain is disrupted in first-episode schizophrenia. NeuroReport 17, 23–26.

Hawkins, K.A., et al., 2004. Neuropsychological status of subjects at high risk for a first episode of psychosis. Schizophr. Res. 67, 115–122.

Hill, K., et al., 2004. Hypofrontality in schizophrenia: a meta-analysis of functional imaging studies. Acta Psychiatr. Scand. 110, 243–256.

Hwang, Y., 2010. Comparisons of estimators of the number of true null hypotheses and adaptive FDR procedures on multiplicity testing. J. Stat. Comput. Simul. 1563–5163.

Jenkinson, M., et al., 2002. Improved optimization for the robust and accurate linear registration and motion correction of brain images. Neuroimage 17, 825–841.

Kay, S.R., et al., 1987. The Positive and Negative Syndrome Scale (PANSS) for schizophrenia. Schizophr. Bull. 13, 261–276.

Latora, V., Marchiori, M., 2001. Efficient behavior of small-world networks. Phys. Rev. Lett. 87, 198701.

Lawrie, S.M., et al., 2002. Reduced frontotemporal functional connectivity in schizophrenia associated with auditory hallucinations. Biol. Psychiatry 51, 1008–1011.

Liu, Y., et al., 2008. Disrupted small-world networks in schizophrenia. Brain 131, 945–961.

Lynall, M.E., et al., 2010. Functional connectivity and brain networks in schizophrenia. J. Neurosci. 30, 9477–9487.

McKiernan, K.A., et al., 2003. A parametric manipulation of factors affecting task-induced deactivation in functional neuroimaging. J. Cogn. Neurosci. 15, 394–408.

Meyer-Lindenberg, A., et al., 2001. Evidence for abnormal cortical functional connectivity during working memory in schizophrenia. Am. J. Psychiatry 158, 1809–1817.

Nelson, H., 1982. National Adult Reading Test (NART). NERT, Windsor.

Ohnuma, T., et al., 1997. A magnetic resonance imaging study in first-episode disorganized-type patients with schizophrenia. Psychiatry Clin. Neurosci. 51, 9–15.

Pantelis, C., et al., 2003. Neuroanatomical abnormalities before and after onset of psychosis: a cross-sectional and longitudinal MRI comparison. Lancet 361, 281–288.

Peters, B.D., et al., 2009. White matter connectivity and psychosis in ultra-high-risk subjects: a diffusion tensor fiber tracking study. Psychiatry Res. 181, 44–50.

Price, G., et al., 2007. Abnormal brain connectivity in first-episode psychosis: a diffusion MRI tractography study of the corpus callosum. Neuroimage 35, 458–466.

Pugliese, E., Castellano, C., 2009. Heterogeneous pair approximation for voter models on networks. EPL 88.

Rubia, K., et al., 2001. An fMRI study of reduced left prefrontal activation in schizophrenia during normal inhibitory function. Schizophr. Res. 52, 47–55.

Rubinov, M., Sporns, O., 2009. Complex network measures of brain connectivity: uses and interpretations. Neuroimage 52 (3), 1059–1069.

Segal, D., et al., 2010. Diffusion tensor anisotropy in the cingulate gyrus in schizophrenia. Neuroimage 50, 357–365.

Sinatra, R., et al., 2010. Optimal Random Walks in Complex Networks with Limited Information. arXiv:1007.4936.
Spence, S.A., et al., 2000. Functional anatomy of verbal fluency in people with schizophrenia and those at genetic risk. Focal dysfunction and distributed disconnectivity reappraised. Br. J. Psychiatry 176, 52–60.
Tan, H.Y., et al., 2007. Dysfunctional and compensatory prefrontal cortical systems, genes and the pathogenesis of schizophrenia. Cereb. Cortex 17 (Suppl. 1), i171–i181.
Turkheimer, F.E., et al., 2001. Estimation of the number of "true" null hypotheses in multivariate analysis of neuroimaging data. Neuroimage 13, 920–930.
van Veen, V., Carter, C.S., 2002. The anterior cingulate as a conflict monitor: fMRI and ERP studies. Physiol. Behav. 77, 477–482.
Wood, S.J., et al., 2008. Progressive changes in the development toward schizophrenia: studies in subjects at increased symptomatic risk. Schizophr. Bull. 34, 322–329.
Yung, A.R., McGorry, P.D., 1996. The prodromal phase of first-episode psychosis: past and current conceptualizations. Schizophr. Bull. 22, 353–370.
Yung, A.R., et al., 2005. Mapping the onset of psychosis: the Comprehensive Assessment of At-Risk Mental States. Aust. NZ J. Psychiatry 39, 964–971.